ADVANCED MATERIALS
www.advmat.de

Cyclodextrin-Derived Intrinsically Bioactive Nanoparticles for Treatment of Acute and Chronic Inflammatory Diseases

Jiawei Guo, Dandan Li, Hui Tao, Gang Li, Renfeng Liu, Yin Dou, Taotao Jin, Lanlan Li, Jun Huang, Houyuan Hu, and Jianxiang Zhang**

Inflammation is a common cause of many acute and chronic inflammatory diseases. A major limitation of existing anti-inflammatory therapeutics is that they cannot simultaneously regulate pro-inflammatory cytokine production, oxidative stress, and recruitment of neutrophils and macrophages. To overcome this limitation, nanoparticles (NPs) with multiple pharmacological activities are synthesized, using a chemically modified cyclic oligosaccharide. The manufacture of this type of bioactive, saccharide material-based NPs (defined as LCD NP) is straightforward, cost-effective, and scalable. Functionally, LCD NP effectively inhibits inflammatory response, oxidative stress, and cell migration for both neutrophils and macrophages, two major players of inflammation. Therapeutically, LCD NP shows desirable efficacies for the treatment of acute and chronic inflammatory diseases in mouse models of peritonitis, acute lung injury, and atherosclerosis. Mechanistically, the therapeutic benefits of LCD NP are achieved by inhibiting neutrophil-mediated inflammatory macrophage recruitment and by preventing subsequent pro-inflammatory events. In addition, LCD NP shows good safety profile in a mouse model. Thus, LCD NP can serve as an effective anti-inflammatory nanotherapy for the treatment of inflammatory diseases mainly associated with neutrophil and macrophage infiltration.

Inflammation, a complex set of interactions between soluble factors and cells, arises in damaged tissues in response to infection and injury.[1] Whereas inflammation is a defense mechanism of the body,[2] uncontrolled/unresolved inflammation directly contributes to the pathogenesis of a diverse array of chronic diseases, such as diabetes,[3] inflammatory bowel disease,[4] infectious diseases,[5] neurodegenerative disease,[6] cardiovascular disease,[7] and immunometabolic disorders.[8] Anti-inflammatory therapy is considered as a promising strategy for the prevention and treatment of these aforementioned diseases.[9,10] Nonsteroidal anti-inflammatory drugs and corticosteroids have been broadly used for the treatment of different inflammatory diseases,[11] despite severe side effects such as gastrointestinal complications,[12] cardiovascular risk,[13] osteoporosis,[14] and aseptic joint necrosis.[15] Biological therapeutics, such as monoclonal antibodies and cytokines, have been used to treat rheumatoid arthritis,[16] Crohn's disease,[17] colitis,[18] atherosclerotic disease,[19] and asthma,[20] by interfering inflammation-associated molecular and cellular processes. Unfortunately, the clinical applications of the biological therapeutics are severely compromised by high cost,[21] loss of response,[22] and risk of serious infections and malignancies.[23] In addition, pro-resolving mediators, including lipoxins, resolvins, protectins, and analogue agents, have been tested in preclinical models of acute and chronic inflammatory diseases.[10,24] However, most of these candidate drugs are still in the proof-of-concept stage and their therapeutic benefits and efficacy remain to be established for disease treatment.[10,25] Therefore, developing innovative strategies and effective new therapies to treat inflammatory diseases is of critical importance.

Recently, anti-inflammatory materials have been investigated as therapeutics against inflammation-associated diseases. For example, nanoparticles (NPs) capable of eliminating reactive oxygen species (ROS) have demonstrated their efficacy in animal models of peritonitis,[26] rheumatoid arthritis,[27] colitis,[28] nonalcoholic steatohepatitis,[29] acute lung injury,[30] sepsis,[31] atherosclerosis,[32] and ischemic stroke.[33] NPs assembled by PEGylated bilirubin can function as a potent anti-inflammatory nanotherapy for the treatment of colitis and asthma,[34] by effectively scavenging ROS and modulating the immune system. Polymer-based NPs that can release free antioxidant molecules by hydrolysis are also efficacious for

Dr. J. W. Guo, D. D. Li, Dr. H. Tao, Dr. G. Li, R. F. Liu, Dr. Y. Dou, T. T. Jin, Dr. L. L. Li, Prof. J. X. Zhang
Department of Pharmaceutics
College of Pharmacy
Third Military Medical University
Chongqing 400038, China
E-mail: jxzhang@tmmu.edu.cn
Dr. J. W. Guo, Prof. H. Y. Hu
Department of Cardiology
Southwest Hospital
Third Military Medical University
Chongqing 400038, China
E-mail: houyuanhu@hotmail.com
Prof. J. Huang
Institute for Molecular Engineering
University of Chicago
Chicago, IL 60637, USA
The ORCID identification number(s) for the author(s) of this article can be found under https://doi.org/10.1002/adma.201904607.

DOI: 10.1002/adma.201904607

the treatment of inflammatory diseases in animal models.[35] Phosphorus-conjugated dendrimers have shown desirable efficacy in treating experimental arthritis and subchronic inflammation induced by zymosan air pouch in mice,[36] by selectively targeting monocytes/macrophages and shaping them toward anti-inflammatory activation. Synthetic dendritic polyglycerol sulfates inhibited leukocyte migration and extravasation to the inflamed tissue, by perturbing adhesive interactions between leukocytes and endothelial cells.[37] In addition, NPs derived from sugar-based amphiphilic polymers could suppress the progression of atherosclerosis, a chronic inflammatory disease.[38] Despite the preliminary success of these anti-inflammatory nanotherapies, their translational applications are still very limited. There are critical needs for developing NPs with defined structure, high quality, and satisfactory safety profile in vivo. Also, mass production of stable, safe, effective, affordable, and pro-resolving NPs for treating inflammation-associated diseases remains a significant challenge.[39]

Herein, we set out to make new NPs for the treatment of inflammation-driven diseases. Because neutrophils and macrophages are major players of both acute and chronic inflammatory diseases,[40] modulating the inflammatory responses of neutrophils and macrophages using NPs represents an intriguing strategy for disease treatment. The mentioned intrinsically bioactive NPs were prepared from a luminol-conjugated β-cyclodextrin (β-CD) (LCD) material using a facile, cost-effective, and scalable approach (**Figure 1**a,b). This nanotherapy (LCD NP) significantly suppressed the production of pro-inflammatory cytokines and oxidative mediators by neutrophils and macrophages as well as dramatically inhibited their migration in vitro. In mouse models of acute and chronic inflammation, including peritonitis, acute lung injury, and atherosclerosis, LCD NP effectively attenuated neutrophil/macrophage-mediated inflammation and demonstrated desirable efficacies and biosafety in treating these inflammatory diseases (Figure 1a).

LCD was synthesized by chemical modification of β-CD (Figure 1b), a cyclic oligosaccharide with seven glucose units linked by α-1,4-glycosidic linkage, which has demonstrated excellent in vivo safety.[41] To this end, β-CD was first activated via 1,1′-carbonyldiimidazole (CDI), and then followed by nucleophilic reaction between luminol and CDI-activated β-CD (Figure S1, Supporting Information). The final product, defined as LCD, was systematically characterized by different measurements. Both Fourier-transform infrared (FTIR) and ^{1}H NMR spectrometry confirmed covalent conjugation of luminol in β-CD (Figure S2a,b, Supporting Information). Additional characterization by matrix-assisted laser desorption/ionization time-of-flight mass spectrometry assured the successful synthesis of LCD (Figure S2c, Supporting Information). According to the ^{1}H NMR spectrum, each LCD molecule has ≈1 luminol and 3 imidazole units. Subsequently, LCD NP was prepared by a nanoprecipitation technique, giving rise to nanoscale particles with spherical shape as illustrated by transmission electron microscopy (TEM) and scanning electron microscopy (SEM) (Figure 1c,d). LCD NP showed a relatively narrow size distribution profile (Figure 1e), with the average hydrodynamic diameter of 238 ± 26 nm and ζ-potential of −31 ± 1 mV in deionized water. In the presence of excessive hydrogen peroxide (H_2O_2), LCD NP was completely hydrolyzed to water-soluble products, including β-CD, imidazole, and 3-aminophthalic acid (Figure S3, Supporting Information). Consequently, LCD NP is degradable under oxidative conditions.

Next, we examined the cellular uptake profiles of LCD NP. Neutrophils isolated from the peritoneal cavity of mice were incubated with Cy5-labeled LCD NP (Cy5/LCD NP). Time-lapse fluorescence microscopy showed a time-dependent cellular internalization profile (**Figure 2**a and Figure S4, Supporting Information). Cellularly, the internalized NPs were mainly transported through the endolysosomal pathways, since the fluorescent signal of Cy5/LCD NP (red) was primarily colocalized with that of LysoTracker (green), which stains late endosomes and lysosomes of cells. As expected, a dose–response uptake profile was observed in neutrophils (Figure S5, Supporting Information). Both time and dose-dependent cellular uptakes were further confirmed by flow cytometric quantification (Figure S6, Supporting Information, and Figure 2b). Similarly, the uptake of Cy5/LCD NP by RAW264.7 murine macrophages was dose and time dependent, as quantified by flow cytometry (Figure S7a,b). Consistently, the endocytosis of Cy5/LCD NP by peritoneal macrophages also showed a dose and time–response pattern (Figure S8, Supporting Information, and Figure 2c,d). Collectively, these results demonstrated that LCD NP could be efficiently internalized by inflammatory cells.

We then investigated the anti-inflammatory activity of LCD NP in vitro. Whereas stimulation of mouse peritoneal neutrophils with phorbol 12-myristate 13-acetate (PMA) led to the production of high-level pro-inflammatory cytokines, such as tumor necrosis factor (TNF)-α and interleukin (IL)-1β, their levels greatly reduced after pretreating neutrophils with LCD NP (Figure 2e,f). Also, pretreatment of neutrophils with LCD NP significantly reduced the generation of oxidative mediators myeloperoxidase (MPO) and ROS stimulated by PMA, respectively (Figure 2g,h and Figure S9a, Supporting Information). Similarly, lipopolysaccharide (LPS)-stimulated inflammatory response and PMA-induced oxidative stress in peritoneal macrophages were significantly attenuated by LCD NP, as shown by the large reduction of TNF-α, IL-1β, and ROS (Figure 2i–k and Figure S9b, Supporting Information) after treatment. For both neutrophils and macrophages, the suppression of inflammatory response by LCD NP was dose dependent (Figure 2e–k). These results showed that LCD NP can effectively inhibit inflammatory response and oxidative stress in inflammatory cells.

Furthermore, LCD NP pretreatment significantly inhibited the migration of RAW264.7 macrophages induced by monocyte chemoattractant protein-1 (MCP-1), in a dose-dependent manner in Transwell assay (**Figure 3**a). Consistently, LCD NP greatly suppressed the migration of RAW264.7 macrophages induced by activated neutrophils (Figure 3b). A similar anti-migration role of LCD NP was also observed in peritoneal macrophages stimulated by either MCP-1 or activated neutrophils (Figure 3c,d). Previous studies have found that the migration and accumulation of inflammatory cells lead to a wide variety of inflammatory diseases.[42] Therefore, pharmacological inhibition of neutrophil-mediated inflammatory monocyte/macrophage recruitment represents a promising approach against both acute and chronic diseases.[43] The results above together implied that LCD NP can serve as an effective

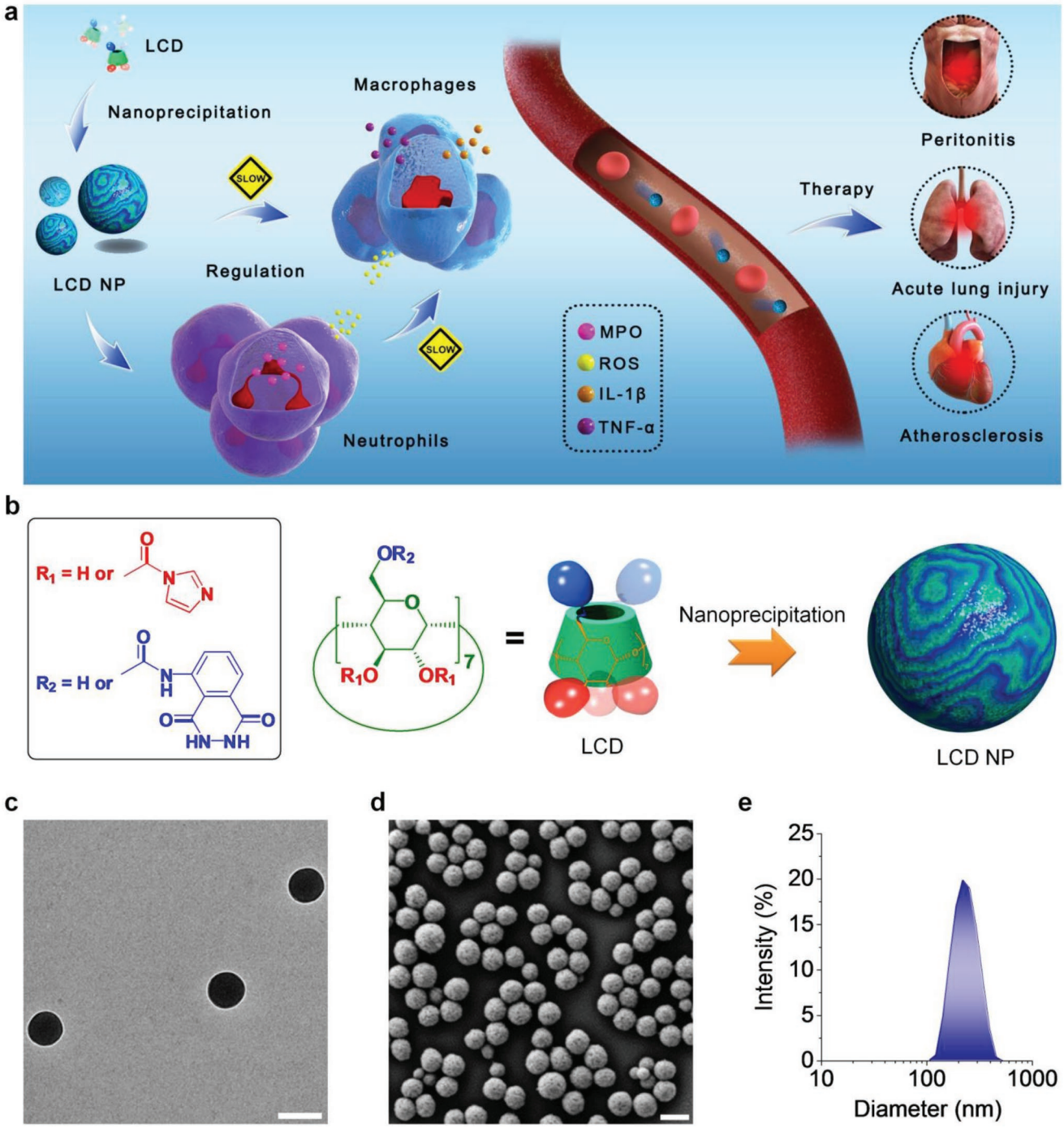

Figure 1. Engineering of anti-inflammatory nanoparticles using β-cyclodextrin. a) A sketch showing the facile development of a nanotherapy for inflammatory diseases by simultaneously regulating neutrophils and macrophages. b) Schematic illustration of the chemical structure of luminol-modified β-cyclodextrin (LCD) and preparation of LCD-derived nanoparticles (LCD NP). c–e) TEM and SEM images as well as the size distribution profile of LCD NP. Scale bars, 200 nm.

anti-inflammatory nanotherapy. Next, we performed in vivo experiments in animal models to test the efficacy and safety of LCD NP.

We first examined the therapeutic potential of LCD NP in typical animal models of acute inflammation. In a zymosan-induced peritonitis mouse model, after 1 h initiation of inflammation, LCD NP was intraperitoneally (i.p.) administered at 4 mg to each mouse (0.12 mmol kg^{-1}). Compared to the saline treated control, LCD NP treatment significantly reduced the production of ROS and inflammatory cytokines TNF-α and IL-1β (**Figure 4**a). We further tested in vivo efficacy of LCD NP in another acute inflammation model of acute lung

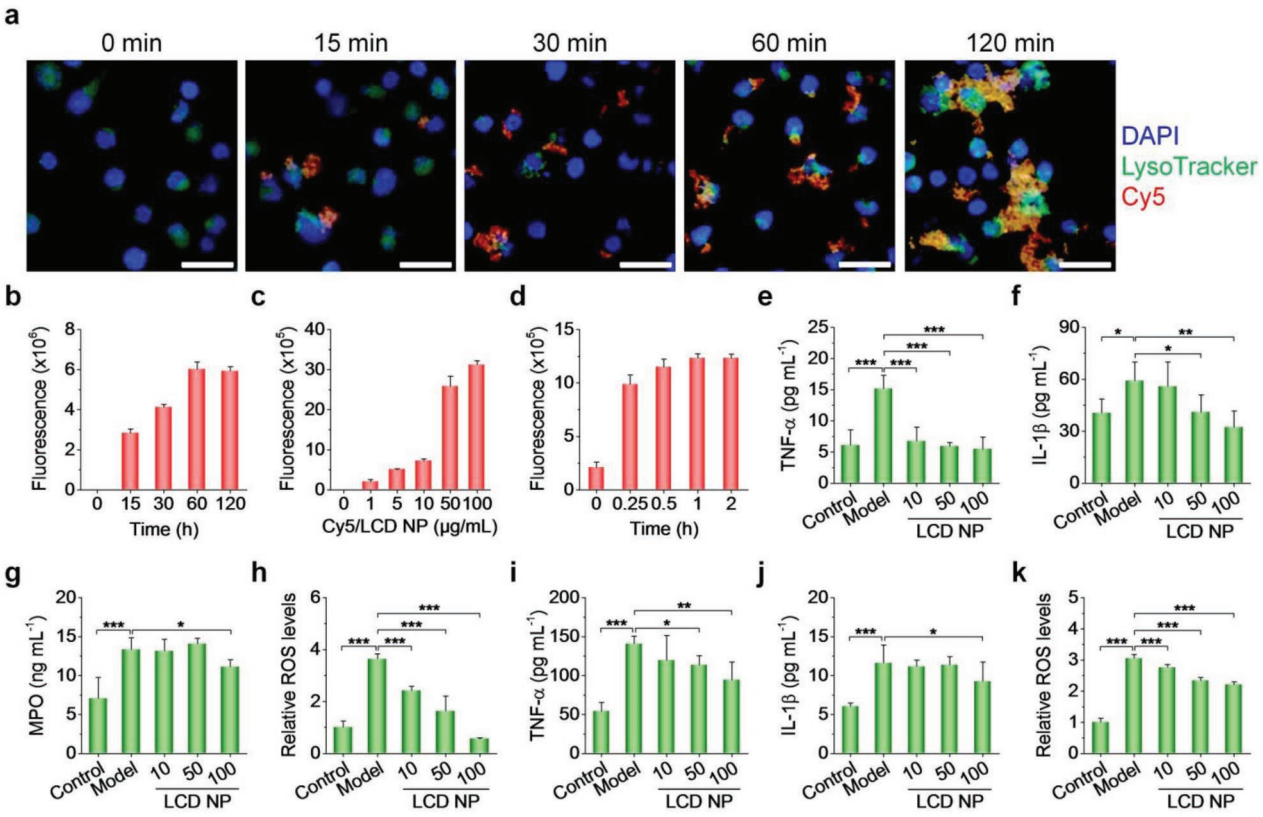

Figure 2. Cellular uptake and in vitro biological effects of LCD NP in peritoneal neutrophils and macrophages. a) Fluorescence images of time-dependent endocytosis of Cy5/LCD NP (red) in neutrophils. Neutrophils were incubated with 50 μg mL^{-1} of Cy5/LCD NP for different times. The endolysosomes were stained with LysoTracker (green) and nuclei were stained with DAPI (blue). Scale bars, 20 μm. b) Intracellular fluorescence intensities of Cy5/LCD NP in neutrophils quantified by flow cytometry. c,d) The cellular internalization of Cy5/LCD NP in peritoneal macrophages in a dose and time-dependent manner. The incubation time was 2 h for dose–response experiments in (c), and 50 μg mL^{-1} Cy5/LCD NP was used for time-dependent studies in (d). e–h) The levels of TNF-α, IL-1β, MPO, and ROS in neutrophils after treatment with fresh medium (control), PMA alone (model), and PMA and various doses of LCD NP (LCD NP), respectively. The relative ROS levels in neutrophils were quantified by flow cytometry using DCFH-DA as a fluorescent probe. i–k) The levels of TNF-α, IL-1β, and ROS in macrophages subjected to various treatments. The treatment protocols were the same as those used for neutrophils. In (e)–(k), the concentration of TPCD NP is expressed as μg mL^{-1}. Data are presented at mean ± s.d. ($n = 5$). *$P < 0.05$, **$P < 0.01$, ***$P < 0.001$.

injury (ALI), which is a major cause of respiratory failure in critically ill patients.[44] ALI in mice was induced by intratracheal inoculation of LPS. After intravenous (i.v.) injection of LCD NP labeled with a near-infrared fluorescent dye Cy7.5, we observed considerable accumulation of Cy7.5 fluorescence in the lung of ALI mice (Figure S10, Supporting Information), indicating that LCD NP targeted the injured lung after i.v. delivery. After treatment with LCD NP via i.v. injection at 2 mg in each mouse (0.06 mmol kg^{-1}), inflammatory responses in the lung were significantly attenuated, as shown by the reduced levels of TNF-α and IL-1β (Figure 4b). Also, LCD NP treatment dramatically reduced the wet-to-dry weight ratio of lung tissues, compared to the model group (Figure 4c). Staining of lungs with Evans Blue further revealed that LCD NP ameliorated pulmonary vascular permeability resulting from local inflammation (Figure 4d). Correspondingly, hematoxylin and eosin (H&E) stained sections also showed attenuated inflammatory cell infiltration and pulmonary edema in mice treated with LCD NP (Figure 4e). These results demonstrated that LCD NP can be used as a nanotherapy for acute inflammation in vivo.

Based on the above promising findings on acute inflammation, we subsequently examined the efficacy of LCD NP for the treatment of atherosclerosis. Increasing evidences have revealed the role of inflammatory cells (such as macrophages and neutrophils) at various stages of atherosclerosis, a chronic inflammatory disorder in the artery.[45] Experimental atherosclerosis was established in apolipoprotein E-deficient (ApoE$^{-/-}$) mice by feeding with a Western diet. Immunofluorescence analysis clearly showed good colocalization between MPO and neutrophils in sections of aortas isolated from mice with atherosclerotic plaques (Figure S11a, Supporting Information). Further flow cytometric quantification indicated that neutrophils significantly increased in the aortic tissue isolated from lesion-bearing ApoE$^{-/-}$ mice (Figure S11b, Supporting Information). Also, the levels of ROS and MPO increased in aortic tissues of the diseased mice (Figure S11c, Supporting Information).

After i.p. administration of Cy7.5-labeled LCD NP, ex vivo imaging revealed strong focal fluorescent signals in the aortic arch and abdominal aorta that are susceptible to the

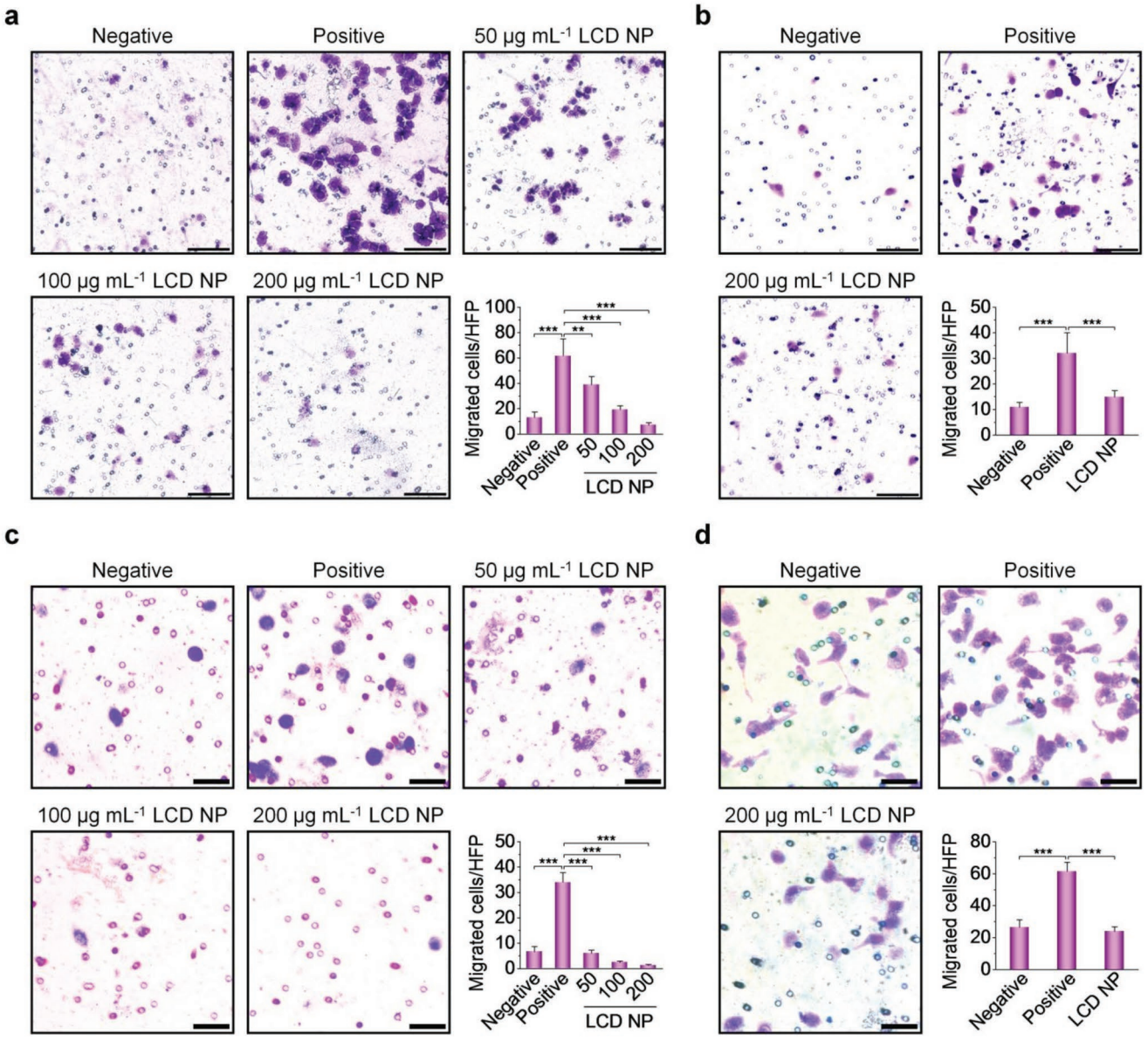

Figure 3. Inhibition of macrophage migration by LCD NP in vitro. a) LCD NP inhibited the in vitro migration of RAW264.7 macrophages induced by MCP-1. Cells were treated by fresh medium (negative), MCP-1 (positive), and the combination of MCP-1 and LCD NP at the concentration of 50, 100, or 200 μg mL^{-1}. b) LCD NP suppressed the migration of RAW264.7 macrophages induced by activated neutrophils. The migration of macrophages in the upper chamber was induced by medium (negative), neutrophils (positive), and the combination of neutrophils and 200 μg mL^{-1} LCD NP in the lower chamber. c) Pretreatment with LCD NP inhibited the migration of peritoneal macrophages induced with MCP-1. d) LCD NP reduced the migration of peritoneal macrophages induced by activated neutrophils. The treatment procedures were the same as those used for RAW264.7 macrophages in (b). Both representative optical microscopy images and quantitative data are presented in each panel. In histograms (a,c), the concentration of TPCD NP is expressed as μg mL^{-1}. Scale bars: 100 μm (a,b), 50 μm (c,d). Data are presented as mean ± s.d. ($n = 5$). $^{**}P < 0.01$, $^{***}P < 0.001$.

development atherosclerosis in ApoE$^{-/-}$ mice (**Figure 5**a), due to the combined effects of low shear stress and disturbed blood flow.[46] This suggested that LCD NP accumulated in atherosclerotic plaques after i.p. delivery. We then examined the therapeutic effects of LCD NP in ApoE$^{-/-}$ mice. After two months of treatment with LCD NP by i.p. administration at 0.6 mg in each mouse (about 18.5 μmol kg^{-1}), we found relatively lowered Oil Red O (ORO)-stained area in the whole aorta (Figure 5b, left panel). Quantitative analysis indicated that the plaque areas of LCD NP-treated mice were significantly smaller than those of control animals (Figure 5b, right panel). Examination on ORO-stained cryosections of the aortic root also showed the reduced plaque formation after LCD NP treatment (Figure 5c). Immunohistochemistry analysis of the plaque composition showed the reduced macrophage number and increased collagen content around plaques in the LCD NP group (Figure 5d,e), while immunofluorescence assay

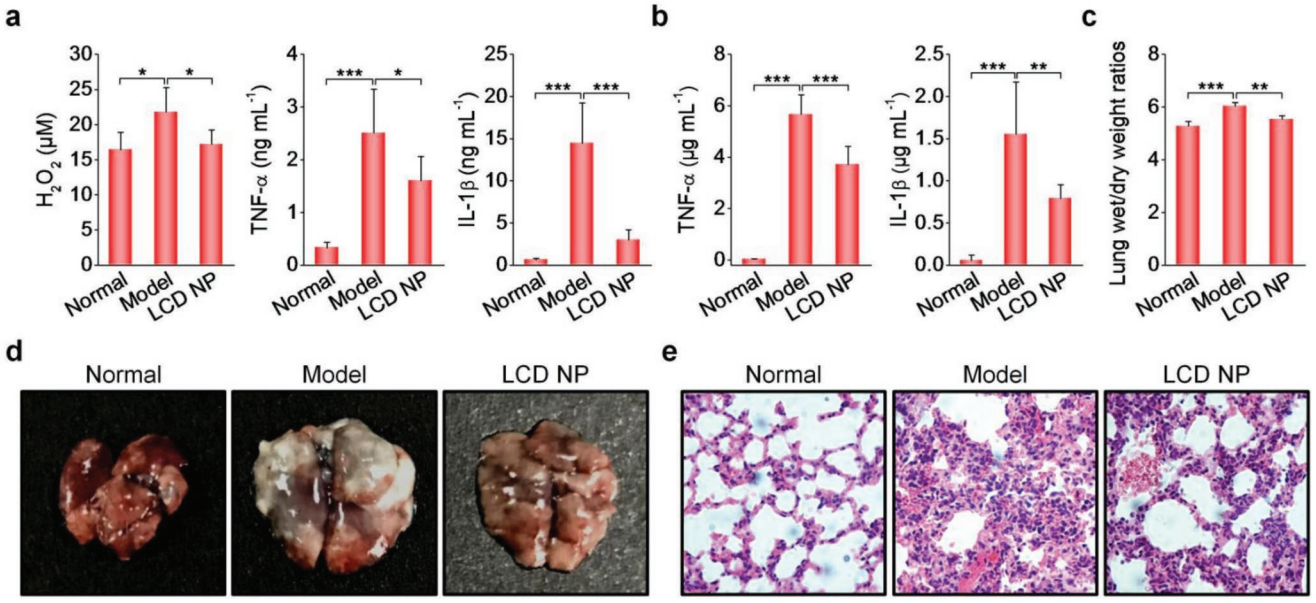

Figure 4. Therapy of acute inflammatory diseases by LCD NP. a) The levels of H_2O_2, TNF-α, and IL-1β in peritoneal exudates of healthy mice (normal), mice with zymosan-induced peritonitis treated with saline (model), and mice with zymosan-induced peritonitis treated with LCD NP (the LCD NP group), respectively. After 1 h zymosan induction, mice were i.p. administered with either saline or LCD NP at 4 mg in each mouse. After 6 h treatment, peritoneal cell-free exudates were analyzed. b) The expression of TNF-α and IL-1β in bronchoalveolar lavage of untreated healthy mice (normal), mice with LPS-induced acute lung injury (ALI) treated with i.v. injected saline (model), and mice with LPS-induced ALI treated with LCD NP (the LCD NP group). c) The lung wet-to-dry weight ratios of mice subjected to different treatments. d) Digital photos of Evans Blue-stained lungs subjected to different treatments. e) H&E sections of lung tissues. 1 h after intratracheal administration of LPS, mice were i.v. administered with LCD NP at 2 mg in each mouse. After 6 h treatment, bronchoalveolar lavage was collected for quantification of different cytokines. In separate experiments, lungs were isolated for additional staining, histological, and quantitative analyses. Data are mean ± s.d. ($n = 6$). $^*P < 0.05$, $^{**}P < 0.01$, $^{***}P < 0.001$.

further revealed remarkably reduced neutrophils and MPO after LCD NP treatment (Figure 5f). Flow cytometry also found significantly reduced neutrophils and macrophages (Figure 5g). As well documented, neutrophils may weaken the fibrous cap by releasing and/or activating different proteinases,[47] and macrophages also positively contribute to the formation of vulnerable plaques.[45] By contrast, the increased content of collagen around plaques is beneficial to plaque stabilization.[48] Taken together, our data demonstrated that LCD NP effectively delayed the development of atherosclerosis and notably enhanced the stability of atheromatous lesions.

Collectively, the above results substantiated that LCD NP may serve as a potential nanotherapy for the treatment of both acute and chronic inflammatory diseases resulting from neutrophil and macrophage infiltration. In addition to systemic delivery, LCD NP can be administered by local injection, such as for the treatment of periodontal disease (a set of inflammatory conditions in periodontal tissues), since previous studies have demonstrated therapeutic advantages of several nanoplatforms.[49] Also, the periodontal treatment might be beneficial for therapy of systemic inflammatory diseases such as diabetes and atherosclerosis in view of their close link with periodontal disease.[50] Moreover, it is possible to further potentiate efficacy of LCD NP by combination therapy with other anti-inflammatory agents.

Finally, we tested the safety profile of LCD NP. During 60 d treatment, LCD NP-treated mice displayed normal body weight gains indistinguishable to those of the untreated control mice (Figure S12a, Supporting Information). Further, the organ index of typical major organs of LCD NP-treated animals was comparable to that of the saline-treated group (Figure S12b, Supporting Information). Representative hematological parameters and biomarkers relevant to liver and kidney functions were in normal levels for all treated mice (Figure S12c,d, Supporting Information), compared to those untreated controls. Additionally, plasma lipids of LCD NP-treated mice were not statistically different from those of the control mice (Figure S12e, Supporting Information). Moreover, H&E staining of major organ pathological sections revealed no discernible destruction of microstructure or inflammatory cell infiltration after LCD NP treatment, compared to untreated controls (Figure S13, Supporting Information). These preliminary results substantiated that LCD NP is safe for long-term administration at the examined dose, although comprehensive studies are necessary to fully demonstrate its in vivo safety.

In conclusion, we have demonstrated that LCD NP is a promising nanotherapy for the treatment of both acute and chronic inflammatory diseases associated with the infiltration of neutrophils and macrophages. Elucidation of molecular and cellular mechanisms underpinning pharmacological activities of

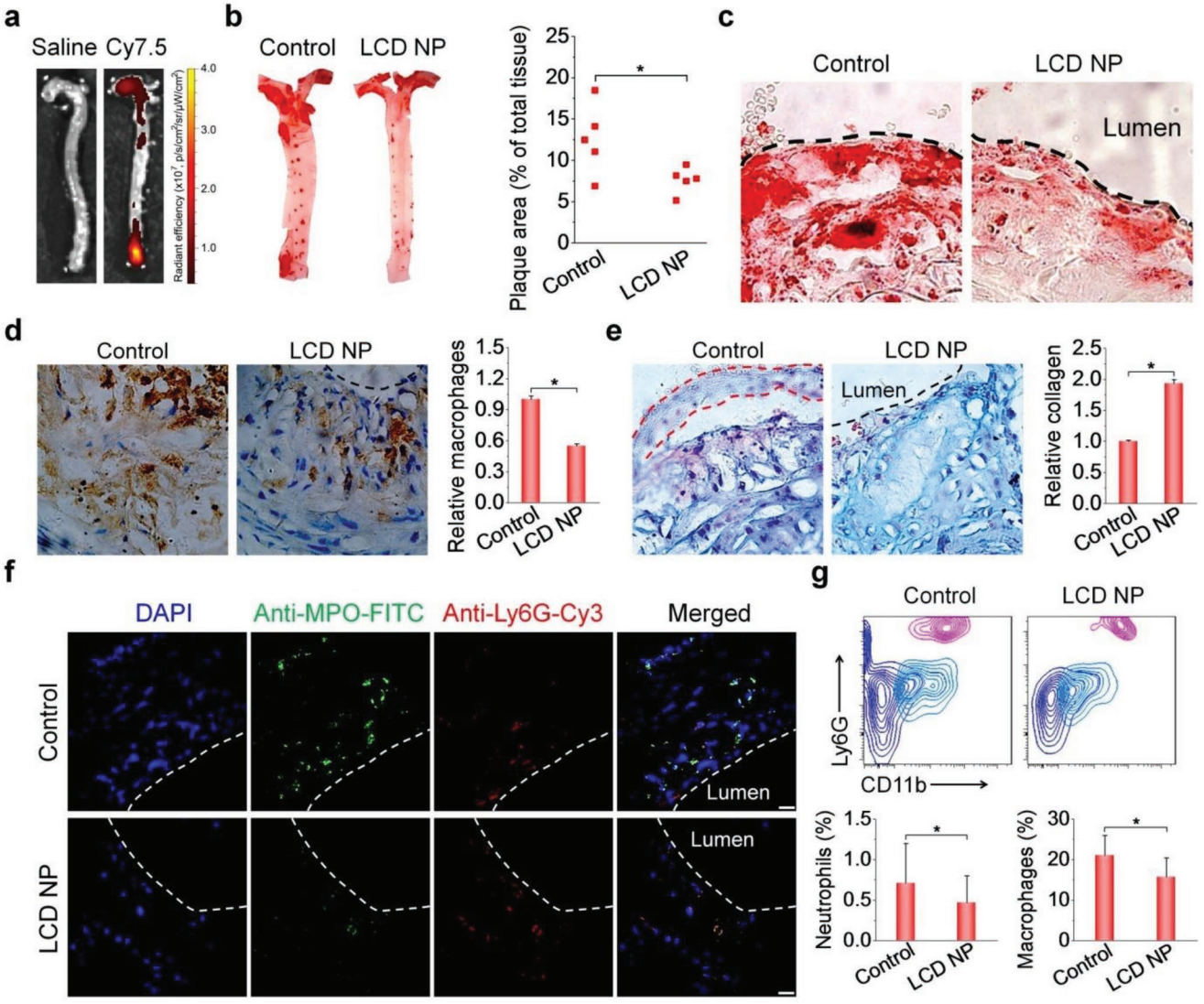

Figure 5. Treatment of atherosclerosis by LCD NP in ApoE$^{-/-}$ mice. a) Ex vivo images showing the accumulation of Cy7.5-labeled LCD NP in the aorta. b) Representative photographs of en face Oil Red O (ORO)-stained total aortas (left) and the corresponding quantification of the lesion area (right). The whole aortas were isolated for analyses after two months of treatment with LCD NP. c) ORO-stained cryosections of aortic roots. d) Representative images (left) and quantification (right) of the macrophage densities by immunohistochemistry analysis of aortic root sections. e) Microscopy images (left) and quantification (right) of the collagen level in the Masson's trichrome-stained sections of aortic roots. f) Immunofluorescence analysis of MPO (green) and neutrophils (red) in aortic sections after treatment with LCD NP. Scale bars, 20 μm. g) Representative flow plots (left) and quantitative histograms (right) showing neutrophil and macrophage frequencies in aortic tissues after treatment with LCD NP. Data are mean ± s.d. ($n = 5$). *$P < 0.05$.

LCD NP can facilitate the development of a new type of anti-inflammatory nanotherapies.

Supporting Information

Supporting Information is available from the Wiley Online Library or from the author.

Acknowledgements

This study was supported by the National Natural Science Foundation of China (Nos. 81801841 and 81971727), the Postdoctoral Science Foundation of China (2018M643863), the Chongqing Special Postdoctoral Science Foundation (XmT2018067), the Innovation Program for Key Technologies of Southwest Hospital (No. SWH2016ZDCX1016), and the Program for Distinguished Young Scholars of TMMU. All animal experiments were performed in line with the Guide for the Care and Use of Laboratory Animals proposed by National Institutes of Health. All procedures and protocols were approved by the Animal Ethics Committee at Third Military Medical University (Chongqing, China).

Conflict of Interest

The authors declare no conflict of interest.

Keywords

bioactive nanoparticles, cyclodextrin, inflammation, macrophages, neutrophils

Received: July 18, 2019
Revised: September 12, 2019
Published online: October 3, 2019

[1] C. Nathan, *Nature* **2002**, *420*, 846.
[2] R. Medzhitov, *Cell* **2010**, *140*, 771.
[3] M. Y. Donath, S. E. Shoelson, *Nat. Rev. Immunol.* **2011**, *11*, 98.
[4] G. G. Kaplan, S. C. Ng, *Gastroenterology* **2017**, *152*, 313.
[5] K. Honda, D. R. Littman, *Annu. Rev. Immunol.* **2012**, *30*, 759.
[6] T. Chitnis, H. L. Weiner, *J. Clin. Invest.* **2017**, *127*, 3577.
[7] P. Libby, J. Loscalzo, P. M. Ridker, M. E. Farkouh, P. Y. Hsue, V. Fuster, A. A. Hasan, S. Amar, *J. Am. Coll. Cardiol.* **2018**, *72*, 2071.
[8] G. S. Hotamisligil, *Nature* **2017**, *542*, 177.
[9] a) I. Tabas, C. K. Glass, *Science* **2013**, *339*, 166; b) N. Ruparelia, J. T. Chai, E. A. Fisher, R. P. Choudhury, *Nat. Rev. Cardiol.* **2017**, *14*, 133.
[10] J. N. Fullerton, D. W. Gilroy, *Nat. Rev. Drug Discovery* **2016**, *15*, 551.
[11] a) J. R. Vane, R. M. Botting, *Am. J. Med.* **1998**, *104*, 2S; b) P. J. Barnes, *Br. J. Pharmacol.* **2006**, *148*, 245.
[12] a) S. E. Gabriel, L. Jaakkimainen, C. Bombardier, *Ann. Intern. Med.* **1991**, *115*, 787; b) I. Bjarnason, J. Hayllar, A. N. d. J. Macpherson, A. N. t. S. Russell, *Gastroenterology* **1993**, *104*, 1832.
[13] P. A. Howard, P. Delafontaine, *J. Am. Coll. Cardiol.* **2004**, *43*, 519.
[14] E. Canalis, *Curr. Opin. Rheumatol.* **2003**, *15*, 454.
[15] A. L. Buchman, *J. Clin. Gastroenterol.* **2001**, *33*, 289.
[16] P. C. Taylor, M. Feldmann, *Nat. Rev. Rheumatol.* **2009**, *5*, 578.
[17] S. R. Targan, S. B. Hanauer, S. J. H. van Deventer, L. Mayer, D. H. Present, T. Braakman, K. L. DeWoody, T. F. Schaible, P. J. Rutgeerts, *N. Engl. J. Med.* **1997**, *337*, 1029.
[18] B. G. Feagan, P. Rutgeerts, B. E. Sands, S. Hanauer, J. F. Colombel, W. J. Sandborn, G. Van Assche, J. Axler, H. J. Kim, S. Danese, I. Fox, C. Milch, S. Sankoh, T. Wyant, J. Xu, A. Parikh, *N. Engl. J. Med.* **2013**, *369*, 699.
[19] P. M. Ridker, B. M. Everett, T. Thuren, J. G. MacFadyen, W. H. Chang, C. Ballantyne, F. Fonseca, J. Nicolau, W. Koenig, S. D. Anker, J. J. P. Kastelein, J. H. Cornel, P. Pais, D. Pella, J. Genest, R. Cifkova, A. Lorenzatti, T. Forster, Z. Kobalava, L. Vida-Simiti, M. Flather, H. Shimokawa, H. Ogawa, M. Dellborg, P. R. F. Rossi, R. P. T. Troquay, P. Libby, R. J. Glynn, *N. Engl. J. Med.* **2017**, *377*, 1119.
[20] M. J. Leckie, A. t. Brinke, J. Khan, Z. Diamant, B. J. O'Connor, C. M. Walls, A. K. Mathur, H. C. Cowley, K. F. Chung, R. Djukanovic, T. T. Hansel, S. T. Holgate, P. J. Sterk, P. J. Barnes, *Lancet* **2000**, *356*, 2144.
[21] I. Khilfeh, E. Guyette, J. Watkins, D. Danielson, D. Gross, K. Yeung, *J. Manag. Care Spec. Pharm.* **2019**, *25*, 461.
[22] S. Vermeire, A. Gils, P. Accossato, S. Lula, A. Marren, *Ther. Adv. Gastroenterol.* **2018**, *11*.
[23] a) Z. A. Borman, J. Cote-Daigneault, J. F. Colombel, *Expert Rev. Gastroenterol. Hepatol.* **2018**, *12*, 1101; b) S. Bonovas, G. Fiorino, M. Allocca, T. Lytras, G. K. Nikolopoulos, L. Peyrin-Biroulet, S. Danese, *Clin. Gastroenterol. Hepatol.* **2016**, *14*, 1385.
[24] C. N. Serhan, *Nature* **2014**, *510*, 92.
[25] C. N. Serhan, N. A. Petasis, *Chem. Rev.* **2011**, *111*, 5922.
[26] Q. Zhang, F. Zhang, Y. Chen, Y. Dou, H. Tao, D. Zhang, R. Wang, X. Li, J. Zhang, *Chem. Mater.* **2017**, *29*, 8221.
[27] J. Kim, H. Y. Kim, S. Y. Song, S. H. Go, H. S. Sohn, S. Baik, M. Soh, K. Kim, D. Kim, H. C. Kim, N. Lee, B. S. Kim, T. Hyeon, *ACS Nano* **2019**, *13*, 3206.
[28] L. B. Vong, T. Tomita, T. Yoshitomi, H. Matsui, Y. Nagasaki, *Gastroenterology* **2012**, *143*, 1027.
[29] A. Eguchi, T. Yoshitomi, M. Lazic, C. D. Johnson, L. B. Vong, A. Wree, D. Povero, B. G. Papouchado, Y. Nagasaki, A. E. Feldstein, *Nanomedicine* **2015**, *10*, 2697.
[30] L. Li, J. Guo, Y. Wang, X. Xiong, H. Tao, J. Li, Y. Jia, H. Hu, J. Zhang, *Adv. Sci.* **2018**, *5*, 1800781.
[31] M. Soh, D. W. Kang, H. G. Jeong, D. Kim, D. Y. Kim, W. Yang, C. Song, S. Baik, I. Y. Choi, S. K. Ki, H. J. Kwon, T. Kim, C. K. Kim, S. H. Lee, T. Hyeon, *Angew. Chem., Int. Ed.* **2017**, *56*, 11399.
[32] Y. Wang, L. Li, W. Zhao, Y. Dou, H. An, H. Tao, X. Xu, Y. Jia, S. Lu, J. Zhang, H. Hu, *ACS Nano* **2018**, *12*, 8943.
[33] C. K. Kim, T. Kim, I. Y. Choi, M. Soh, D. Kim, Y. J. Kim, H. Jang, H. S. Yang, J. Y. Kim, H. K. Park, S. P. Park, S. Park, T. Yu, B. W. Yoon, S. H. Lee, T. Hyeon, *Angew. Chem., Int. Ed.* **2012**, *51*, 11039.
[34] a) Y. Lee, H. Kim, S. Kang, J. Lee, J. Park, S. Jon, *Angew. Chem., Int. Ed.* **2016**, *55*, 7460; b) D. E. Kim, Y. Lee, M. Kim, S. Lee, S. Jon, S. H. Lee, *Biomaterials* **2017**, *140*, 37.
[35] a) B. R. Cho, D. R. Ryu, K. S. Lee, D. K. Lee, S. Bae, D. G. Kang, Q. Ke, S. S. Singh, K. S. Ha, Y. G. Kwon, D. Lee, P. M. Kang, Y. M. Kim, *Biomaterials* **2015**, *53*, 679; b) S. Kannan, H. Dai, R. S. Navath, B. Balakrishnan, A. Jyoti, J. Janisse, R. Romero, R. M. Kannan, *Sci. Transl. Med.* **2012**, *4*, 130ra46.
[36] a) M. Hayder, M. Poupot, M. Baron, D. Nigon, C. O. Turrin, A. M. Caminade, J. P. Majoral, R. A. Eisenberg, J. J. Fournie, A. Cantagrel, R. Poupot, J. L. Davignon, *Sci. Transl. Med.* **2011**, *3*, 81ra35; b) I. Posadas, L. Romero-Castillo, N. El Brahmi, D. Manzanares, S. Mignani, J. P. Majoral, V. Ceña, *Proc. Natl. Acad. Sci. USA* **2017**, *114*, E7660.
[37] J. Dernedde, A. Rausch, M. Weinhart, S. Enders, R. Tauber, K. Licha, M. Schirner, U. Zugel, A. von Bonin, R. Haag, *Proc. Natl. Acad. Sci. USA* **2010**, *107*, 19679.
[38] D. R. Lewis, L. K. Petersen, A. W. York, K. R. Zablocki, L. B. Joseph, V. Kholodovych, R. K. Prud'homme, K. E. Uhrich, P. V. Moghe, *Proc. Natl. Acad. Sci. USA* **2015**, *112*, 2693.
[39] C. D. Buckley, D. W. Gilroy, C. N. Serhan, *Immunity* **2014**, *40*, 315.
[40] a) S. K. Jorch, P. Kubes, *Nat. Med.* **2017**, *23*, 279; b) E. Kolaczkowska, P. Kubes, *Nat. Rev. Immunol.* **2013**, *13*, 159; c) F. K. Swirski, M. Nahrendorf, *Science* **2013**, *339*, 161; d) L. Honold, M. Nahrendorf, *Circ. Res.* **2018**, *122*, 113; e) J. W. Williams, C. Giannarelli, A. Rahman, G. J. Randolph, J. C. Kovacic, *J. Am. Coll. Cardiol.* **2018**, *72*, 2166.
[41] a) J. Guo, H. Tao, Y. Dou, L. Li, X. Xu, Q. Zhang, J. Cheng, S. Han, J. Huang, X. Li, X. Li, J. Zhang, *Mater. Today* **2017**, *20*, 493; b) M. E. Davis, M. E. Brewster, *Nat. Rev. Drug Discovery* **2004**, *3*, 1023; c) J. X. Zhang, P. X. Ma, *Adv. Drug Delivery Rev.* **2013**, *65*, 1215.
[42] a) E. F. Morand, *Intern. Med. J.* **2005**, *35*, 419; b) A. D. Luster, R. Alon, U. H. von Andrian, *Nat. Immunol.* **2005**, *6*, 1182.
[43] O. Soehnlein, L. Lindbom, C. Weber, *Blood* **2009**, *114*, 4613.
[44] A. M. Manicone, *Expert Rev. Clin. Immunol.* **2009**, *5*, 63.
[45] K. J. Moore, I. Tabas, *Cell* **2011**, *145*, 341.
[46] Y. Nakashima, A. S. Plump, E. W. Raines, J. L. Breslow, R. Ross, *Arterioscler. Thromb.* **1994**, *14*, 133.
[47] O. Soehnlein, *Circ. Res.* **2012**, *110*, 875.
[48] C. Silvestre-Roig, M. P. de Winther, C. Weber, M. J. Daemen, E. Lutgens, O. Soehnlein, *Circ. Res.* **2014**, *114*, 214.
[49] a) M. Y. Mahmoud, J. M. Steinbach-Rankins, D. R. Demuth, *J. Controlled Release* **2019**, *297*, 3; b) C. Ni, J. Zhou, N. Kong, T. Bian, Y. Zhang, X. Huang, Y. Xiao, W. Yang, F. Yan, *Biomaterials* **2019**, *206*, 115; c) X. Bao, J. Zhao, J. Sun, M. Hu, X. Yang, *ACS Nano* **2018**, *12*, 8882.
[50] a) P. M. Preshaw, A. L. Alba, D. Herrera, S. Jepsen, A. Konstantinidis, K. Makrilakis, R. Taylor, *Diabetologia* **2012**, *55*, 21; b) W. G. Haynes, C. Stanford, *Arterioscler., Thromb., Vasc. Biol.* **2003**, *23*, 1309.

